Sensitivity of Satellite Retrievals of Temperature to Errors in Estimates of Tropospheric Water Vapor

MICHAEL P. WEINREB

National Environmental Satellite Service, NOAA, Washington, D.C. 20233

(Manuscript received 28 September 1976, in revised form 22 April 1977)

ABSTRACT

A priori estimates of the vertical distribution of tropospheric water vapor are needed to solve the radiative transfer equation in the 15 μm CO_2 band to derive tropospheric temperatures from radiances measured at orbiting satellites. This paper shows how errors in estimates of water vapor mixing ratio propagate into these solutions for temperature, and in simulation establishes the sensitivity of the rms errors in a collection of temperature soundings from the NOAA 2 satellite to errors in mixing ratio. The simulations predict that errors found in available estimates of mixing ratio degrade the solutions for temperature in the low troposphere so that they provide little new information over that already in the forecasts of the National Meteorological Center.

1. Introduction

Atmospheric temperature profiles can be deduced from satellite measurements of radiance through a solution of the radiative transfer equation in the 15 μm CO_2 band. The atmospheric variables that enter the solution algorithm, such as the amount and distribution of water vapor, must be estimated beforehand. However, our estimates of these quantities for use in temperature soundings are not accurate. For example, it will be shown in Section 4 that estimates of water vapor mixing ratio for use in temperature retrievals from the Vertical Temperature Profile Radiometer (VTPR) instruments (McMillin *et al.*, 1973) are subject to errors which often exceed 30% of the values measured by nearby radiosondes.

Section 2 describes how errors in estimates of mixing ratio are propagated into the solution for temperature. Section 3 shows in simulation how sensitive to these errors are the accuracy and information content of a collection of temperature soundings. Section 4 presents data on errors in the estimates of mixing ratio used in actual temperature soundings. With this information the simulations predict the accuracy and information content for a collection of temperature soundings that are subject to no errors except those in mixing ratio.

This work is confined to solutions of the radiative transfer equation in the 15 μm band of CO_2. It does not include solutions in the 4.3 μm band of CO_2. Also, it applies only to temperature retrievals by methods that use the radiative transfer equation. It does not apply to regression methods.

2. Propagation of error into the solution for temperature

Water vapor enters the radiative transfer equation through its effects on atmospheric transmittances and their derivatives with respect to altitude, the weighting functions. Although the calculations of transmittances in the spectral intervals of the VTPR near 15 μm are dominated by the spectral lines of CO_2, they also include the spectral lines of water vapor and the continuum of water vapor that overlap the CO_2 features. For a description of how the weighting functions are computed for the VTPR, see McMillin *et al.* (1973) and Wark *et al.* (1974).

Fig. 1 shows weighting functions for VTPR channels 5 (725 cm^{-1}) and 6 (747 cm^{-1}) for an atmosphere sounded by radiosonde at Midway Island on 1 March 1973. The temperature and water vapor profiles are shown in Fig. 2. The solid curves in Fig. 1 are the weighting functions computed for this atmosphere in the two channels. To demonstrate the sensitivity of the weighting functions to changes in the amount of water vapor, we recomputed the weighting functions for the same atmosphere with the mixing ratio increased at each level by 25%. These are the dashed curves in Fig. 1. The effect of increasing the amount of water vapor has been to raise the weighting functions in the atmosphere. In general, then, errors in *a priori* estimates of water vapor produce errors in weighting functions in the 15 μm region.

VTPR radiances for the Midway Island atmosphere were simulated by integration of the radiation transfer

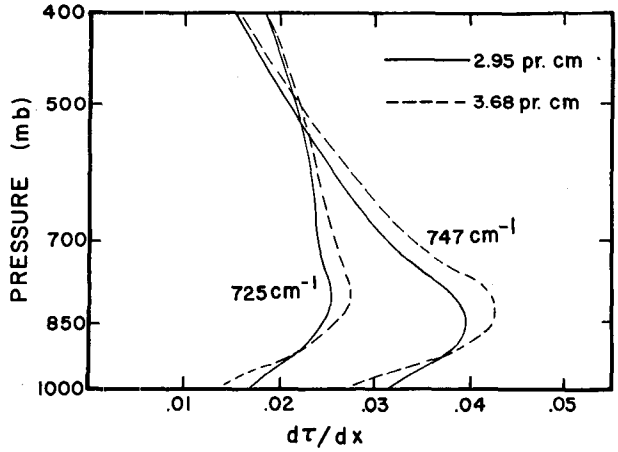

FIG. 1. Weighting functions for two VTPR channels for two amounts of water vapor. The parameter x is proportional to altitude. The abbreviation pr. cm refers to precipitable water in centimeters.

equation to test their sensitivity to changes in mixing ratio. Radiances for the four channels sensing the troposphere are shown in Fig. 3. The "correct" mixing ratio (see Fig. 2) was used to produce the radiances at zero "Excess mixing ratio". The radiances at other values of "Excess mixing ratio" correspond to mixing ratios changed by the percentages shown. For example, this figure shows that errors up to 25% in estimated mixing ratio, which, as we shall see in Section 4 are not unusually large, cause errors up to 1.3 mW sr^{-1} m^{-2} cm^{1} in the computed radiance in the VTPR channel at 747 cm^{-1}. Such errors have major effects on the accuracies of temperature retrievals.

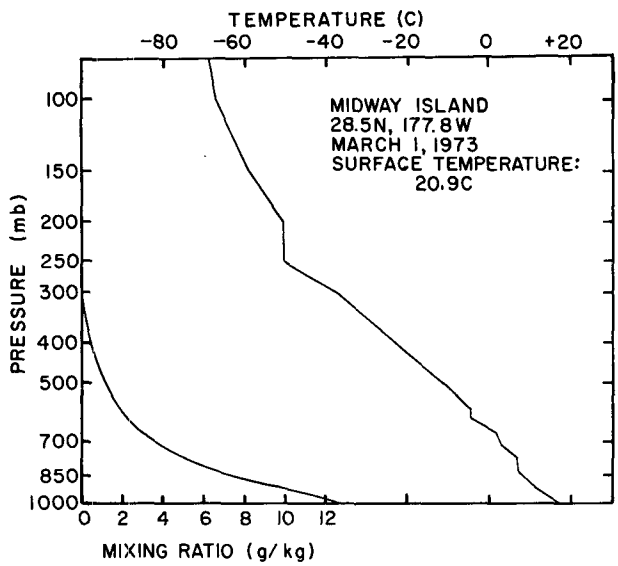

FIG. 2. Temperature and mixing ratio profiles at Midway Island, 1 March 1973. Scale for temperature is at top, for mixing ratio at bottom.

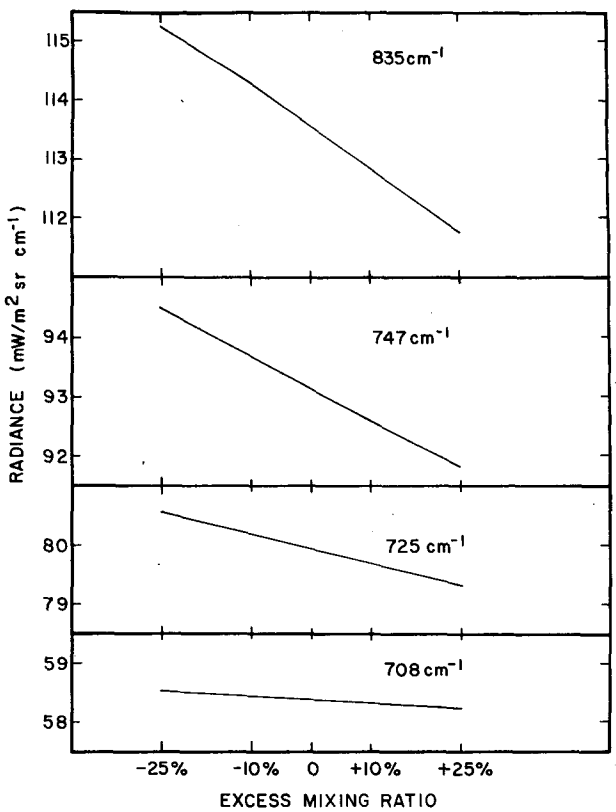

FIG. 3. VTPR radiances vs changes in mixing ratio.

To show this, retrievals were performed by the minimum-information method (Fleming and Smith, 1972) on the set of radiances simulated from the Midway Island sounding. One retrieval assumed the correct mixing ratio profile in constructing transmittances. Four other retrievals, with the assumed mixing ratio changed by $\pm 10\%$ and $\pm 25\%$, were also performed. No other sources of error were present. Fig. 4 shows the profiles of retrieval-radiosonde differences for the five retrieved temperature profiles. These differences vary systematically with the assumed mixing ratio profile. For example, a 25% change in assumed mixing ratio causes about a 2°C change in the retrieved temperatures at 1000 and 850 mb. (Note that the retrieval with the correct profile of mixing ratio is several degrees too warm at 1000 and 850 mb. This is caused by the structure of the initial estimate of temperature used in the retrieval, which is over 5°C warmer than the radiosonde sounding at these levels.)

How does the minimum-information solution propagate errors in mixing ratio through the retrieval algorithm? The minimum information algorithm (Fleming and Smith, 1972) is

$$B = B_0 + \sum_{i=1}^{6} C_i \Delta R_i, \qquad (1)$$

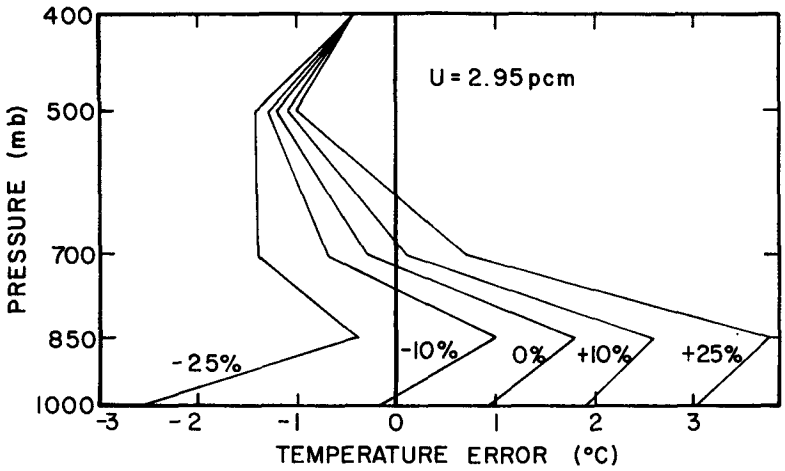

FIG. 4. Profiles of errors of retrieved temperatures vs changes in mixing ratio. The abbreviation pcm refers to precipitable water in centimeters.

where B and B_0 are, respectively, the solution and the initial estimate for the Planck function at any level of the atmosphere; the C_i are the coefficients of the inverse operator; and the ΔR_i are the differences between the measured radiances and the radiances calculated from the initial profile. The index i runs from 1 to 6, representing the VTPR's six channels in the 15 μm CO_2 band.

The mixing ratio enters this solution both in C_i and ΔR_i, because both C_i and ΔR_i depend on the weighting functions, which in turn depend on the mixing ratio. Designating by $\delta(\ )$ the change in a quantity caused by changing the mixing ratio, one derives from Eq. (1) the following expression for $\delta(B)$, the change in the solution:

$$\delta(B)=\sum_{i=1}^{6} C_i\delta(\Delta R_i)+\sum_{i=1}^{6}\delta(C_i)\Delta R_i+\sum_{i=1}^{6}\delta(C_i)\delta(\Delta R_i).$$

The first term on the right side of this equation represents the change in B caused by a change in the calculated radiances, with the C_i remaining unchanged. The second term is the change in B caused by a change in the solution coefficients, with the calculated radiances unchanged. The third term contributes only when both C_i and ΔR_i change.

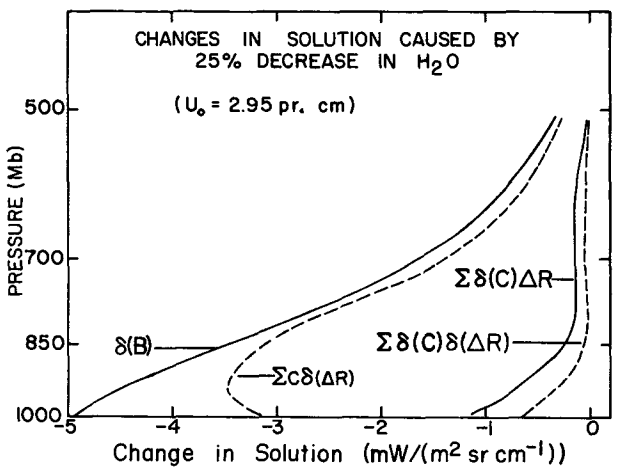

FIG. 5. Components of the change in retrieved Planck-function profile $[\delta(B)]$ for a 25% decrease in the mixing ratio.

Figs. 5 and 6 show the components of $\delta(B)$ caused by a 25% decrease (Fig. 5) and a 25% increase (Fig. 6) in the mixing ratio used in the Midway Island retrieval. From these figures we can conclude that changes in the assumed mixing ratio affect the temperature chiefly through changes in the calculated radiances. The effect of changes in the inverse operator is secondary.

3. Simulation with ensembles of soundings

a. Entire Northern Hemisphere

Up to now we have considered the effects of water vapor on a single sounding. Next we turn to a study in simulation of the effect of errors in estimates of water vapor on an ensemble of temperature retrievals. The study is based on 139 different atmospheres for which a VTPR overpass and a radiosonde launch came within 110 mi and 3 h of each other. All of the 139 atmospheres occurred in March 1973, and all were located over oceans between the latitudes of 18°N and 70°N. In the simulations, the "measured" radiances were computed from the temperature profiles measured by radiosonde, mixing-ratio profiles derived by regression on the radiosonde temperatures (Weinreb and Crosby, 1973), and surface temperatures from the VTPR archives of March 1973 (McMillin *et al.* 1973). These "measured" radiances were uncorrupted by instrument errors or the effects of clouds. We obtained the retrievals in the simulation by the minimum-information algorithm [Eq. (1)], with the initial estimates of the temperatures coming from the forecasts made by the National Meteorological Center. These initial temperatures were identical to those used in the operational VTPR processing. It

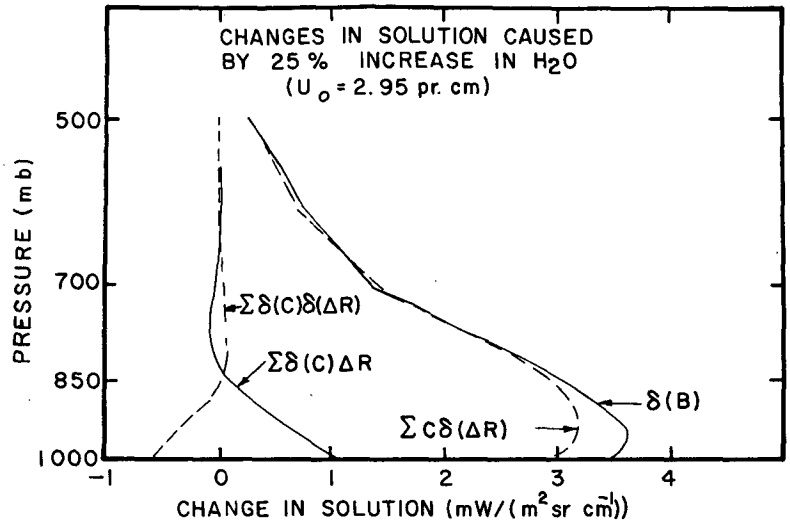

FIG. 6. As in Fig. 5 except for a 25% increase in the mixing ratio.

should be kept in mind that the initial temperatures are used in Eq. (1) to compute not only B_0, but also the transmittances and, hence, the coefficients C_i.

The entire set of 139 retrievals was performed many times, and the only changes from one set to the next were in the water vapor mixing ratio profiles used in constructing transmittances for Eq. (1). The initial temperatures and measured radiances were not changed. Thus the effects of changing the accuracy of the assumed mixing ratio profiles were isolated.

The set of 139 retrievals was done first with the correct profile of mixing ratio, i.e., the profile used in constructing the radiances. A second set of retrievals was performed next with *incorrect* profiles of mixing ratio constructed as follows. If we designate the correct profile of mixing ratio by $\mathbf{W}_0$, which is a vector quantity, then the incorrect profile $\mathbf{W}$ is given by

$$\mathbf{W}=\mathbf{W}_0(1+x), \tag{2}$$

where x, a scalar, is a normally distributed random variable with zero mean and with an rms (σ_x) of 0.125. In other words, for each of the 139 soundings x takes a different value, but the rms of all these values is 0.125, and the mean is zero. The elements of $\mathbf{W}$ were never allowed to exceed the value at saturation. In Section 4 it will be seen that this behavior of $\mathbf{W}$ is similar to that of the assumed mixing ratio in operational retrievals.

Finally, the set of retrievals was performed four more times, each set similar to the second set, except that σ_x, the rms value of x, was increased to 0.250, 0.375, 0.500 and 0.625. Thus, when this was completed, there were six sets of 139 retrievals—one with the correct mixing-ratio profile and five with erroneous mixing ratio profiles given by Eq. (2) with the five different values of σ_x.

For future reference, note that the quantity ρ, defined by $\rho=100\,\sigma_x$, is the rms percent error in mixing ratio.

The results of these simulations will be shown in several forms. First, the rms errors for the whole set of 139 retrievals are shown in Fig. 7. Here the term "error" means the difference between the retrieved temperature and the radiosonde temperature. Each column in the figure represents a profile (versus pressure) of rms errors in the retrieved temperatures corresponding to the value of ρ on the abscissa. Looking across a row at a given pressure, one sees the increase in rms error of the retrievals as the error in water vapor (measured by ρ) increases. The contours of integer values of the rms retrieval error are also drawn in.

The leftmost column of Fig. 7 is noteworthy. It is the profile of rms errors resulting from minimum-information solutions employing transmittances based on the correct mixing-ratio profiles. Furthermore, these solutions are not affected by such problems as instrument noise, clouds in the field of view, bad estimates of sur-

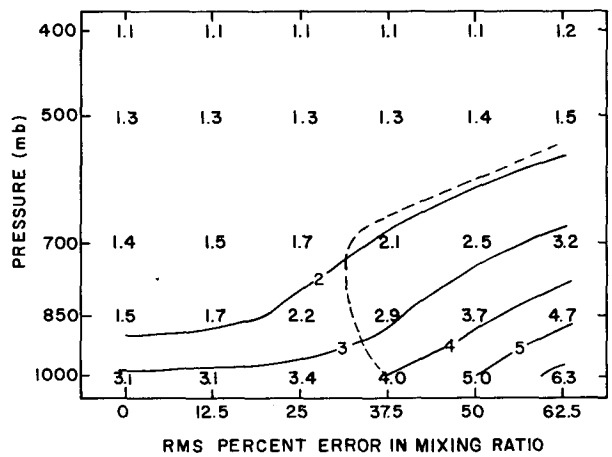

FIG. 7. Profiles of rms temperature error vs rms percent error in the mixing ratio for 139 VTPR soundings in the Northern Hemisphere, March 1973.

face temperatures, etc. In other words, these are the best solutions that we can extract from the VTPR data of March 1973, as long as we apply the minimum-information algorithm and use forecasts for the initial temperatures and for calculating transmittances. Nevertheless, these solutions have nonzero errors, which in fact range from 1–3°C in rms. The errors are caused chiefly by the fundamental difficulties with Fredholm equations of the first kind (Phillips, 1962).

The remaining data in Fig. 7 show that as the error in mixing ratio increases, so does the error in the retrieved temperature profile, particularly at the levels below 500 mb. The dashed line is the locus of points where the rms temperature error of the retrievals equals the rms error of the initial temperatures. Thus in the area above and to the left of this line, the retrievals are more accurate than the initial temperatures. However, for $\rho \gtrsim 35\%$, the retrievals at 700 mb and below have a larger rms error than the initial temperatures.

Even if the retrievals have larger rms errors than the initial temperatures, they may still be useful if they provide some information lacking in the initial temperatures. The source of this new information, if it exists, will be the measured radiances. One measure of the new information is an index proposed by D.S. Crosby of NOAA-NESS (private communication) and briefly described here. For any pressure level, a linear combination T_C of retrieved temperature T_R and initial temperature T_I can be formed; i.e.,

$$T_C = aT_R + (1-a)T_I,$$

where the constant a is determined from the requirement that the rms error in T_C be minimized over a large sample of soundings. The retrievals provide new information if the rms error of T_C is less than that of T_I. Letting R_C and R_I be respectively the rms errors of T_C and T_I, one defines the information-content index

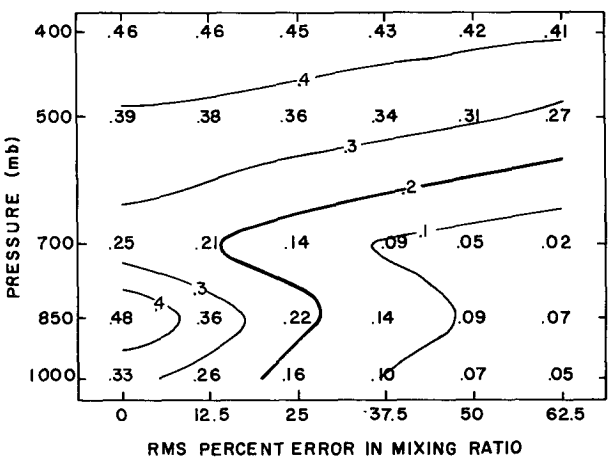

FIG. 8. Profiles of information content index vs rms percent error in the mixing ratio for 139 VTPR soundings in the Northern Hemisphere, March 1973.

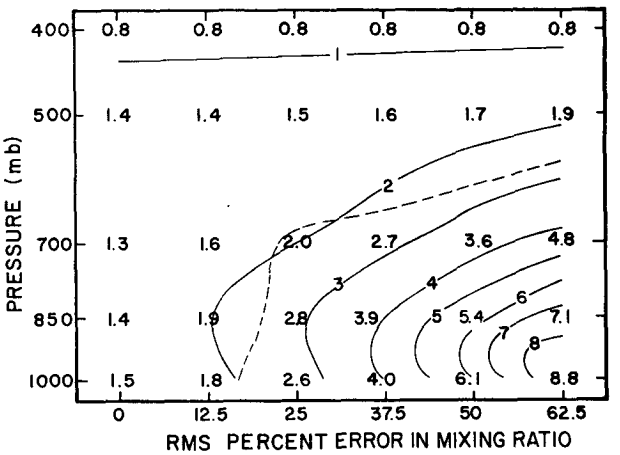

FIG. 9. As in Fig. 7 except for 25 VTPR soundings, 0–20 °N. Average total precipitable water in zone is 3.71 cm.

ICI by,

$$\mathrm{ICI} = 1 - R_C/R_I.$$

If the retrievals add no new information, then $R_C = R_I$, and the ICI is zero. If the new information in the retrieved temperatures causes T_C to be error-free, then $R_C = 0$, and the ICI is unity. Usually the ICI takes values between 0 and 1. The higher its value, the more new information there is in the sample of retrievals.

The values of ICI for the retrievals on the set of 139 atmospheres are shown in Fig. 8, which is similar in construction to Fig. 7. The contours here represent even tenths in the value of the ICI. It is noteworthy that no value of the ICI shown in Fig. 8 exceeds 0.5, even for retrievals with no sources of error ($\rho = 0$).

Because the values of the ICI are statistically significant only to 0.1 or 0.2 for a sample of this size, we have adopted the criterion that the ICI must exceed 0.2 if a significant amount of new information is to be provided by the retrievals. Hence the contour at this value in Fig. 8 has been accentuated. With this criterion, Fig. 8

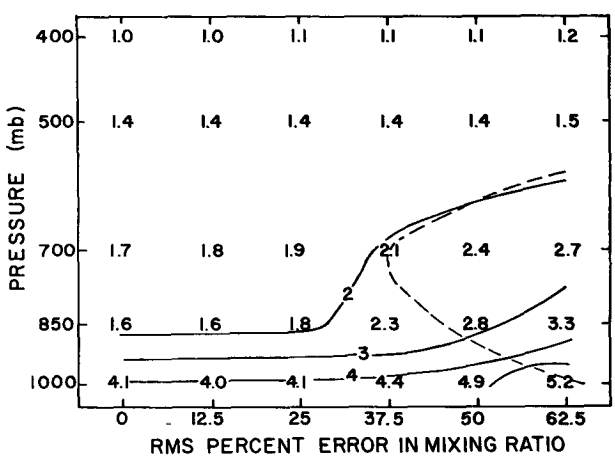

FIG. 10. As in Fig. 9 except for 50–60 °N. Average total precipitable water in zone is 0.96 cm.

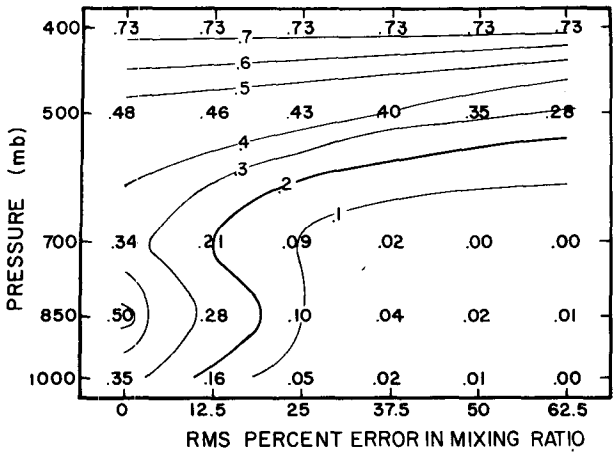

FIG. 11. Profiles of information content index vs rms percent error in the mixing ratio for 25 VTPR soundings, 0–20 °N, March 1973. Average total precipitable water in zone is 3.71 cm.

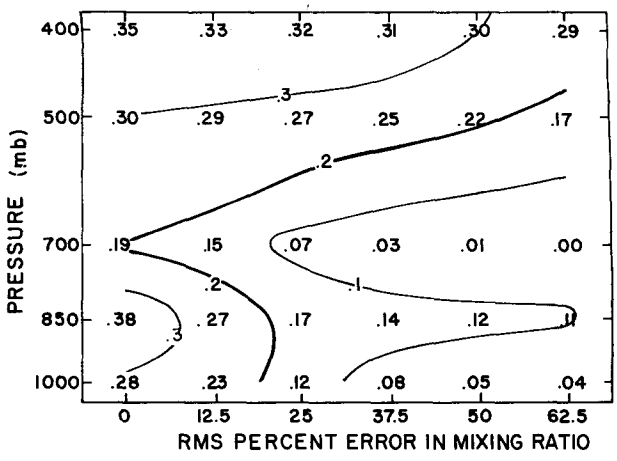

FIG. 13. Profiles of information content index vs rms percent error in mixing ratio for errors in initial profiles between 1 and 2°C.

shows that the retrievals will not provide much information at 700 mb and below unless the value of ρ is less than about 20%. That is, the mixing ratio has to be more accurate than 20% for the retrieved temperatures to contain new information.

b. *Dependence on latitude*

The importance of water vapor in the retrievals is not the same at all latitudes. Figs. 9 and 10, which are constructed like Fig. 7, illustrate the sensitivity of rms temperature errors to ρ in the 0–20°N and 50–60°N zones of latitude, respectively. In each zone the statistics cover 25 soundings. Figs. 11 and 12 show the sensitivity of the ICI to ρ in the same two zones. At 0–20°N, the retrievals at 700 mb and below will not be useful once $\rho > 20\%$, as measured both by the rms error and the ICI. In fact, according to Fig. 10 the retrievals are more accurate than the initial estimates until $\rho \gtrsim 50\%$. One also notes from Figs. 9 and 11 that with increasing ρ the soundings at 0–20°N are degraded more drastically than those at 50–60°N.

The explanation for the different behavior in the two zones is based on the fact that ρ measures percent error in mixing ratio. Hence a given value of ρ produces a larger error in units of mixing ratio—and consequently a larger error in the temperature retrieval—at 0–20°N, where mixing ratios are high, than at 50–60°N, where mixing ratios are low.

c. *Dependence on accuracy of initial estimate of temperature*

Another way of looking at the results of the foregoing simulations is shown in Figs. 13 and 14. At each level of the atmosphere the soundings were grouped according to the accuracy of the initial estimate of tempera-

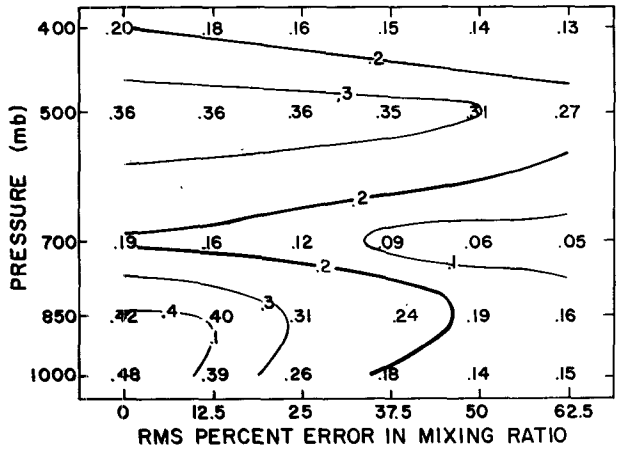

FIG. 12. As in Fig. 11 except for 50–60 °N. Average total precipitable water in zone is 0.96 cm.

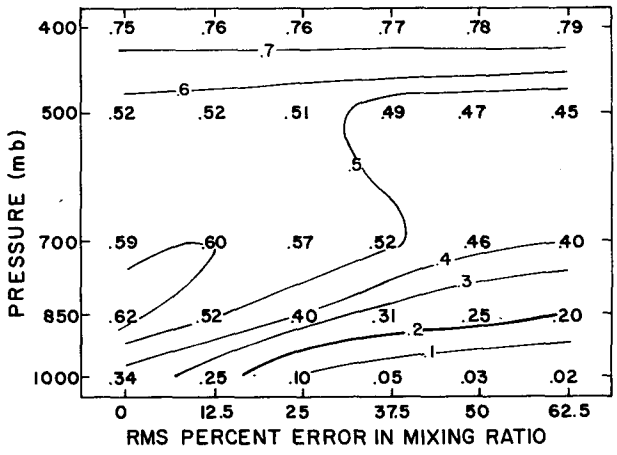

FIG. 14. As in Fig. 13 except for errors in initial profiles between 3 and 4°C.

ture. With accurate initial estimates, it should be difficult for the retrievals to provide much information as measured by the ICI. Conversely, when the initial estimates have large errors, the retrievals should add much information. Fig. 13 shows the sensitivity of the ICI to increases in ρ for the soundings of the full sample of 139 where the errors of the initial estimates fall between 1 and 2°C, which is a small error. Fig. 14 shows the same thing for initial estimates with large errors, falling between 3 and 4°C. By comparing the columns with $\rho=0$ in the two figures, we can see that the retrievals do indeed provide less new information when the initial estimates are more accurate. Furthermore, when the errors of the initial estimates fall between 1 and 2°C, it takes only a small value of ρ ($\sim$15%) to make the amount of new information added at 700 mb and below nearly negligible. On the other hand, much larger values of ρ can be tolerated when the errors of the initial estimates fall between 3 and 4°C.

In the next section it is shown that values of ρ encountered in actual soundings far exceed 15%. Therefore, for this sample of soundings we should not expect the retrievals to provide new information in the subsample where the errors of the initial estimates are less than 2°C.

4. Comparison with an ensemble of real soundings

To place the results of the preceding section in perspective, we need to know something about the distribution of errors of mixing ratio profiles used in real soundings. In the preceding simulations, for any value

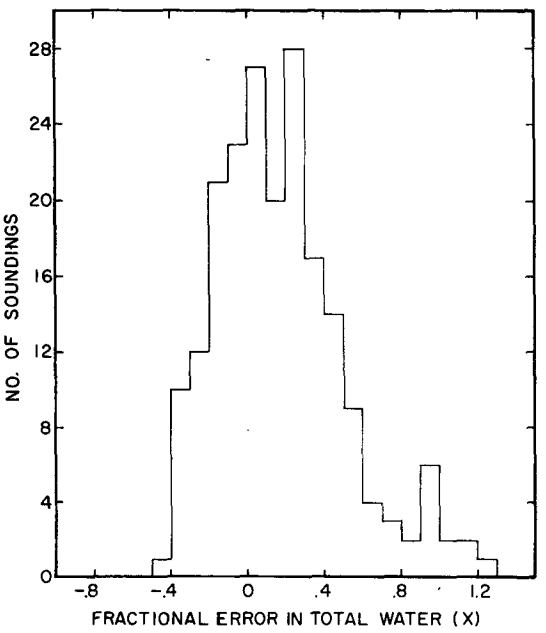

FIG. 15. Histogram of fractional error in total amount of water vapor, from operational VTPR soundings, March 1973.

TABLE 1. Root-mean-square percent error (ρ) in total precipitable water.

Latitude	0–20°N	50–60°N	Entire Northern Hemisphere
ρ(%)	30	40	45

of σ_x, individual values of x were produced on the computer with a normally distributed random number generator. Eq. (2) was then applied to produce the assumed, erroneous profiles **W**. One effect of this procedure was that for any profile, the ratio $(1+x)$ between the assumed and true mixing ratios was the same at all levels of the atmosphere. This characteristic approximates the real situation sometimes but not always.

Another characteristic of the simulations was that x took a different value for each sounding, and its distribution was normal and unbiased. For a comparison of this behavior with that of real soundings, the values of x for the operational minimum-information soundings in the Northern Hemisphere in March 1973 were computed by

$$x=(U_I-U_{rs})/U_{rs}, \tag{3}$$

where U_I and U_{rs} are the total precipitable water, respectively, for the water vapor profile used in the retrievals and for the profile measured by the radiosonde, which is assumed to be the "truth." Fig. 15 is a histogram of the number of soundings whose x values fall in a given interval. The distribution of x is roughly normal, as expected, with a standard deviation of 0.45. However, the distribution has a bias of 0.19, whereas the distribution in simulation was unbiased.

From the data of Fig. 15 one can derive a value for ρ, namely 45%. The bias in x has been ignored because its behavior, which includes latitudinal and seasonal dependences, is not easy to simulate. Table 1 shows values of ρ for the two latitude zones 0–20°N and 50–60°N, and for the whole Northern Hemisphere. These values of ρ are very high, perhaps higher in fact than the true values of ρ, because they contain an extra

TABLE 2. Root-mean-square temperature errors and ICI values from simulations, Northern Hemisphere, March 1976.

	Latitude					
	0–20°N (ρ=25%)		50–60°N (ρ=35%)		0–70°N (ρ=40%)	
Pressure (mb)	rms (°C)	ICI	rms (°C)	ICI	rms (°C)	ICI
1000	2.6	0.05	4.3	0.20	4.2	0.09
850	2.8	0.10	2.1	0.25	3.1	0.13
700	2.0	0.09	2.1	0.10	2.2	0.08
500	1.5	0.43	1.4	0.35	1.3	0.33
400	0.8	0.73	1.1	0.15	1.1	0.43

TABLE 3. As in Table 2 except for real VTPR soundings.

Pressure (mb)	Latitude 0–20°N rms (°C)	0–20°N ICI	50–60°N rms (°C)	50–60°N ICI	0–70°N rms (°C)	0–70°N ICI
1000	2.9	0.04	4.4	0.17	3.7	0.10
850	3.8	0.01	2.9	0.04	3.4	0.01
700	2.1	0.08	2.9	0.02	2.4	0.04
500	1.8	0.24	2.4	0.18	2.0	0.12
400	1.6	0.42	2.2	0.23	1.8	0.18

amount of variability caused, for example, by differences in space and time between the trajectory of the radiosonde and the column under the satellite used to estimate U_I.

In Figs. 7–12 one can read the profiles of rms error and ICI predicted by the simulations for realistic values of ρ equal to (or slightly smaller than) the values in Table 1. For example, from Fig. 9 and the value $\rho=25\%$ we expect temperature errors in the 0–20°N zone to be about 2.6, 2.8 and 2.0°C, respectively, at 1000, 850 and 700 mb. These errors, which are also listed in the first column of Table 2, are all larger than the rms errors of the initial estimates (dashed line in Fig. 9). Hence the simulations predict that with realistic errors in water vapor, the retrievals at 700 mb and below will not be as accurate as the initial profiles in the 0–20°N zone. The ICI values for this zone for $\rho=25\%$ can be read from Fig. 11 and are listed in the second column of Table 2. No value at 700 mb and below exceeds 0.10, implying that the retrievals at these levels add little information to that already in the initial estimates.

At 50–60°N the situation is not so bad. For $\rho=35\%$, Fig. 10 shows that the rms errors of the retrievals are smaller than those of the initial profiles. However, the ICI values at 700 mb and below, determined from Fig. 12 and appearing in the fourth column of Table 2, exceed 0.2 only at the 850 mb level. Thus, taking the rms errors and the ICI values together, the simulations predict that these retrievals at 50–60°N are slightly useful at 700 mb and below.

The preceding predictions of rms errors and ICI values are summarized in Table 2 for 0–20°N and 50–60°N. Similar predictions for all the soundings in the Northern Hemisphere (0–70°N) are also included. It is interesting to compare these values with the actual rms errors and ICI values for the operational VTPR retrievals of the same month (March 1973), which appear in Table 3. The operational rms errors should tend to be larger than the simulated rms errors, and the operational ICI values should tend to be lower than the simulated values, since sources of error other than just water vapor affect the operational retrievals. This expectation is borne out by a comparison of Tables 2 and 3.

5. Conclusion

The simulations in this paper show that tropospheric temperature soundings made by the minimum-information algorithm from VTPR radiance measurements are highly sensitive to errors in the estimates of mixing ratio of water vapor. This sensitivity decreases with increasing latitude in the Northern Hemisphere. When realistic errors in estimated mixing ratio are considered, the simulations predict that the soundings at 700 mb and below add little in rms accuracy or information content to the initial profiles. This conclusion holds at all latitudes in the Northern Hemisphere. At the lower latitudes, where the effects of water vapor are greatest, the simulations predict that the soundings provide no new information. These predictions are consistent with the operational VTPR results of March 1973.

Errors in the assumed water vapor mixing ratio are propagated into the retrieved solutions principally through calculations of radiances from the initial profiles. This fact suggests an approach for future study to reduce the sensitivity of retrievals to errors in the assumed mixing ratio; that is, to try to arrange that the errors in the measured radiances be equal to the errors in the calculated radiances. Then in the retrieval procedure [Eq. (1)] the two errors will cancel when the differences between measured and calculated radiances are formed. Some cancellation may be already occurring because of the way "clear" radiances are being inferred from cloud-contaminated measurements in the current VTPR processing (see McMillin *et al.*, 1973). In this procedure the errors in clear radiances often are nearly proportional to the errors in the radiance calculated at 835 cm^{-1}. On the other hand, Fig. 3 shows that the errors in the calculated radiances are also nearly proportional to the errors in the radiance calculated at 835 cm^{-1}. Thus within the factor ΔR_i in Eq. (1) there should be a partial cancellation of errors arising from errors in the assumed water vapor. Such considerations suggest that the coupling of errors from clouds and water vapor is a worthwhile subject for future study.

Acknowledgment. This work is part of a comprehensive study at NESS of satellite soundings in simulation, which Dr. Sigmund Fritz, now at the University of Maryland, initiated. I also thank Dr. Fritz for many informative and useful discussions.

REFERENCES

Fleming, H. E., and W. L. Smith, 1972: Inversion techniques for remote sensing of atmospheric temperature profiles. *Temperature: Its Measurement and Control in Science and Industry*, H. H. Plumb, Ed., Vol. 4, Part 3, Instrum. Soc. Amer., 2239–2250.

McMillin, L. M., D. Q. Wark, J. M. Siomkajlo, P. G. Abel, A. Werbowetzki, L. A. Lauritson, J. A. Pritchard, D. S. Crosby,

H. M. Woolf, R. C. Luebbe, M. P. Weinreb, H. E. Fleming, F. E. Bittner and C. M. Hayden, 1973: Satellite infrared soundings from NOAA spacecraft. NOAA Tech. Rep. NESS 65, National Environmental Satellite Service, Washington, D.C., 112 pp.

Phillips, D. L., 1962: A technique for the numerical solution of certain integral equations of the first kind. *J. Assoc. Comp. Mach.*, **9**, 84–97.

Wark, D. Q., J. H. Lienesch and M. P. Weinreb, 1974: Satellite observations of atmospheric water vapor. *Appl. Opt.*, **13**, 507–511.

Weinreb, M. P., and D. S. Crosby, 1973: Estimation of atmospheric moisture profiles from satellite measurements by a combination of linear and nonlinear methods. *Preprints Third Conf. Probability and Statistics in Atmospheric Science*, Boulder, Amer. Meteor. Soc., 231–235.